Field amplified sample stacking of amyloid beta (1-42) oligomers using capillary electrophoresis

Sadia Paracha and Christa Hestekin
Ralph E. Martin Department of Chemical Engineering, University of Arkansas, Fayetteville, Arkansas 72701, USA

(Received 2 April 2016; accepted 1 June 2016; published online 15 June 2016)

Oligomeric forms of the amyloid beta (Aβ) protein have been indicated to be an important factor in the development of Alzheimer's disease (AD). Since the oligomeric forms of Aβ can vary in size and conformation, it is vital to understand the early stages of Aβ aggregation in order to improve the care and treatment of patients with AD. This is the first study to determine the effect of field amplified sample stacking (FASS) on the separation of oligomeric forms of A$\beta_{1\text{-}42}$ using capillary electrophoresis (CE) with ultraviolet (UV) detection. UV-CE was able to separate two different species of A$\beta_{1\text{-}42}$ oligomers (<7 mers and 7–22 mers). Although FASS required the use of a higher ionic strength buffer, A$\beta_{1\text{-}42}$ oligomers had the same aggregation behavior as under the non-FASS conditions with only small changes in the amounts of oligomers observed. In general, FASS provided smaller peak widths (>75% average reduction) and increased peak heights (>60% average increase) when compared to non-FASS conditions. UV-CE with FASS also provided higher resolution between the A$\beta_{1\text{-}42}$ oligomers for all aggregation time points studied. In addition, Congo red and Orange G inhibition studies were used to help evaluate the conformation of the observed species. This work demonstrates the ability of UV-CE employing FASS to provide higher resolution between oligomeric forms of A$\beta_{1\text{-}42}$ without significantly altering their aggregation. *Published by AIP Publishing.* [http://dx.doi.org/10.1063/1.4954051]

I. INTRODUCTION

As discoveries within the human proteome have increased, misfolded proteins and mutations of numerous proteins are being linked with various disorders (such as Alzheimer's, Parkinson's, Type II Diabetes, etc.) in today's world.[1–5] Misfolded proteins have the potential to interact with one another creating toxic aggregates, amyloids, which are most commonly known for fibril accumulation and an increase in β-sheet content.[1,2] Alzheimer's disease (AD) is a devastating progressive neurodegenerative disease without any current preventative treatment. AD is the most common form of dementia with the number of deaths increasing by 71% between 2000 and 2013.[4,6] It is estimated that for 2015 the total cost in health care for Americans with AD will be $226 billion.[6] As the population continues to increase in life span, AD patient cases will also increase, creating a huge economic and social impact in the near future.[3,6]

Though the exact mechanism of the disease is still unclear, AD has been correlated with a wide range of cytotoxic aggregated amyloid beta (Aβ) structures.[1,7–9] A$\beta_{1–40}$ has been found at higher physiological concentrations, but A$\beta_{1–42}$ is more pathogenic and predominantly found in the Aβ plaques.[3,7,10–14] A$\beta_{1–40}$ and A$\beta_{1–42}$ vary by two hydrophobic amino acids in the C-terminus, isoleucine and alanine, leading A$\beta_{1–42}$ to be more aggregation prone and to having a higher toxicity.[14,15] Furthermore, studies have been conducted showing that decreasing the A$\beta_{1–42}$ level leads to a reduction in the risk of developing AD.[15,16] Recent studies have also shown that AD can occur without the presence of fibril plaques and suggest that the small soluble Aβ oligomers are the likely neurotoxic agent that is associated with the progress of

AD.[1,6,9–12,17–20] The formation of oligomers are believed to be intracellular and can potentially affect synapse functions, disruption of glutamate uptake, and prevent the ability to maintain proper memory.[1,3,17,21] Since the oligomer aggregates are unstable and time dependent, the exact shape, size, and pathological pathway are hard to determine.[22,23]

A variety of techniques, including native page, enzyme-linked immunosorbent assay, light scattering, mass spectrometry, and size exclusion chromatography, have been used to study Aβ as reviewed in depth by Pryor *et al.*[24] Many previous studies have highlighted the difficulty in narrowing the type of intermediate aggregates formed (such as ADDLs (amyloid beta-derived diffusible ligands), oligomers <30 kDa, fibrillar oligomer, and protofibrils) and in analyzing Aβ without causing alternative aggregate pathways due to experimentation.[3,6,14,17,19,25] Capillary electrophoresis (CE) offers the ability to rapidly analyze these species at high resolution without the use of denaturants or organic solvents which have been reported to alter the Aβ kinetics.

CE uses a uniform electric field to separate proteins based on their conformation and size, which typically correlates with molecular weight. Fig. 1 shows the general set-up for CE. The negatively charged surface of the capillary leads to a bulk flow called electro-osmotic flow (EOF). Under the conditions used in this study, the amyloid beta aggregates have a negative charge which is opposite the direction of the EOF. Capillary coatings are often used to reduce protein adsorption to the walls as well as to suppress EOF. Key advantages of CE include rapid analysis times, low sample volume requirements, and the ability to use a variety of pre-concentration techniques.

CE dimensions are typically 50–100 μm with sample volumes of microliters but actual injection volumes as low as a few nanoliters.[26] CE-based separations have also been translated to microchip and nanochip formats to allow for more rapid separations, lower sample volumes, as well as the ability create a total analysis platform or lab-on-a-chip.[27–29]

Capillary electrophoresis has previously been used to study amyloid beta aggregation. Sabella *et al.* detected Aβ_{1-40} and Aβ_{1-42} oligomers (up to dodecamers) and larger aggregates using CE with ultraviolet (UV) detection and an SDS (sodium dodecyl sulfate) rinse.[30] Picou *et al.* used UV-CE to separate Aβ_{1-42} monomer from fibrils.[31] Kato *et al.* used CE with laser induced fluorescence (LIF) to separate two different Aβ_{1-42} aggregates.[32] Brambilla *et al.* used LIF-CE to show that Aβ_{1-42} aggregation is altered in the presence of PEGylated nanoparticles.[33] Furthermore, Pryor *et al.* used UV-CE to demonstrate the differences in Aβ_{1-40} oligomer aggregation depending on how the samples are prepared.[34] Although electrophoresis in microfluidic chips has been used to study the amyloid beta protein, thus far it has not been used to study its aggregation.[35] Additionally, while these studies have indicated the value and potential for using capillary or microchip electrophoresis to improve our understanding of

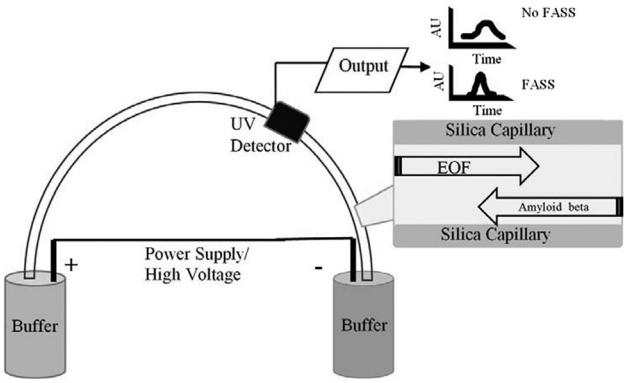

FIG. 1. Representative schematic of the capillary electrophoresis detection. Electro-osmotic flow (EOF) moves toward the cathode, while the negatively charged amyloid beta aggregates move toward the anode. The capillary coating is used to decrease EOF, but does not completely eliminate it. The UV detector output the absorbance over time for the FASS and non-FASS analyses.

amyloid beta aggregation, they have not examined how sample pre-concentration methods might improve the detection of amyloid beta oligomer species.

One simple method of sample stacking that has been reported to increase sensitivity up to at least 10 fold for peptide samples is field amplified sample stacking (FASS).[26,36–40] FASS involves injecting a sample at a lower buffer concentration (load buffer) than the separation (or background electrolyte, BGE). Since the field strength is inversely proportional to conductivity, ions in the load buffer migrate faster than ions in the BGE. When the load buffer ions reach the interface with the BGE, they stack due to the slower migration of the BGE. Therefore, FASS can be used to increase the limit of detection and the resolution for detection of a sample. This is the first study to demonstrate the ability of FASS to detect $A\beta_{1–42}$ oligomers with a higher resolution than non-FASS conditions while not altering the aggregation kinetics. Therefore, UV-CE implementing FASS offers the potential to observe more oligomeric peaks with increased sensitivity.

II. MATERIALS AND METHODS

A. Aβ sample preparation

A 1 mg lyophilized powder of $A\beta_{1–42}$ sample from AnaSpec (San Jose, CA, USA) was pretreated using 1,1,1,3,3,3-hexafluoro-2-propanol (HFIP) as described by Pryor *et al*.[34] The pretreated sample was separated into vials, dried, and stored at −80 °C. In order to analyze $A\beta_{1–42}$, the HFIP treated peptide was solubilized in 5 mM NaOH and kept on ice for 10 min. After 10 min, enough sodium phosphate buffer with pH = 7.4 was added to the sample to reach the desired final concentration. The sample solution was kept on ice for an additional 20 min. When needed, samples were analyzed using a spectrophotometer at 277 nm to verify concentration (using Beer's law with extinction coefficient of 1280 l/(mol*cm)). Congo red and Orange G experiments were conducted using 16.7 μM stock solution of inhibitor where 2% of the total sample volume was the inhibitor. This concentration was based on the findings by Necula *et al* and Pryor *et al*.[34,41] Congo red and Orange G were dissolved in deionized water to make the stock solution.

B. CE studies

All studies were conducted at 25 °C using UV detection on P/ACE MDQ Glycoprotein System from Beckman Coulter, Inc., with a 214 nm filter, the total capillary length of 31 cm, and the length to detector of 10 cm. All fused silica capillary tubing were purchased from Polymicro Technologies with an inside diameter of 51 μm. The $A\beta_{1–42}$ samples were pressure injected at 0.5 psi for typically 8 s and separated at 7 kV. The separation buffer (also called background electrolyte or BGE) for the CE was 100 mM sodium phosphate buffer with pH = 7.4.

In order to coat the capillary, the capillary was equilibrated by conducting a preconditioning wash on a new capillary that included a 0.1 M NaOH rinse, a di-water rinse, and a 0.1 M HCl rinse to potentially wash away adsorbed substances on the capillary wall and regenerate the capillary. The capillary was coated using 0.5% 2000 kDa poly(ethylene) oxide (PEO) purchased from Sigma Aldrich. The PEO coating helped reduce interactions between the capillary and $A\beta_{1–42}$ and also suppressed electroosmotic flow. Additionally, the high molecular weight coating provided a strong hydrophilic/neutral environment for peptide separation and had self-coating properties. In addition, a polymer separation matrix was used in each run to enhance the separation of the electrophoretic peaks. The polymer separation matrix consisted of 0.5% 50 kDa PEO dissolved in the 100 mM sodium phosphate buffer pH = 7.4 and 0.1% of 0.1% 2000 kDa PEO. Once the capillary was coated, the capillary was utilized for at most 4 days depending on the amount of sample analyzed. Before each sample injection, the capillary was washed with filtered di-water to clean out contaminants and the coating was regenerated with the polymer matrix. The polymer coating can break down over time or have decreased efficiency due to protein adsorption. Therefore, a long wash followed by rinsing with polymer matrix (which contains a small amount of coating polymer) is believed to increase the lifetime of the capillary.[42]

C. Aggregation study

All amyloid beta aggregation studies utilized a VWR micro plate shaker at 25 °C and 300 RPM. At 0, 2, 4, 7, 12, 18, 24, and 27 h, 20 μl of the Aβ_{1-42} in either 100 mM (n = 3) or 40 mM sodium phosphate buffer (n = 4) was used for the CE experimentations and 3 μl was used for transmission electron microscopy (TEM) imaging (n = 1 for each buffer). Data collected by the CE were analyzed to determine the migration time and absorbance intensity. The CE data were translated from 32 Karat using Excel VBA program and compared using Origin® (64 bit) from OriginLab Corporation. A bi-Gaussian fit was used to calculate the migration time, peak area, width, and height.

In order to estimate oligomer size, the Aβ_{1-42} samples were centrifuged using Nanosep MF centrifugal filters (Pall Life Science) where the filtrate was analyzed using the CE. The centrifugation process was conducted at 4 °C. Initial experiments indicated that there was noticeable loss of the protein onto the filters, and therefore, the sample concentration was increased from 30 μM to 60 μM. The 60 μM Aβ_{1-42} aggregated samples at 0 h and 7 h were analyzed. Before filtering 20 μl of the 60 μM Aβ_{1-42} sample was analyzed using CE to determine that there were no significant changes in the peak pattern due to the increase in concentration. The rest of the sample was filtered through one of the filters (30 kDa, 100 kDa, or 300 kDa).

In parallel with the ThT assays at 300 RPM, a parafilm sheet was dotted with 3 μl of 30 μM Aβ_{1-42} at 0, 12, 27, 51, and 79 h for TEM imaging, n = 1 for each buffered (40 mM or 100 mM) amyloid. Additionally, 20 μl of 30 μM Aβ_{1-42} inhibited by either Congo red or Orange G was studied using the CE at 0, 2, 4, 7, 12, 18, 24, and 27 h. TEM imaging was also conducted at 0, 12, 27, and 51 h for both inhibitors, n = 2.

III. RESULTS AND DISCUSSION

A. Time-frame for Aβ_{1-42} oligomer formation

It was first necessary to establish an experimental time-frame where oligomer formation would be expected. The time for Aβ_{1-42} oligomer formation was estimated by conducting a thioflaving-T (ThT) binding assay along with observations using transmission electron microscopy (TEM). ThT binds to aggregate with β-sheet conformations, which are believed to occur after the formation of toxic oligomeric species. Similarly, TEM can be used to visualize fibrils, which also occur after the formation of oligomers. Because of the difficulty in observing oligomeric species without alterations, these two methods were used to determine an upper time limit for experiments. An agitation rate of 300 RPM was selected for the study as it allowed a lag time up to 7 h before the formation of β-sheets as detected by ThT binding (see supplementary material).[43] TEM images revealed the first fibril formation at approximately 27 h of aggregation, which also correlated with a decrease in fluorescent intensity in the ThT binding curves (see supplementary material).[43] Therefore, the upper time limit for the aggregations studies was 27 h.

B. UV-CE with and without FASS

FASS provides a simple method to improve the separation and resolution of species detected using UV-CE. Preliminary studies with bovine serum albumin were used to determine an optimum FASS sample buffer concentration of 40 mM sodium phosphate (data not shown). As shown in Fig. 2, the UV-CE analysis with both non-FASS (a) and FASS (b) conditions consisted of more than one species of Aβ_{1-42} as indicated by the presence of two distinct peaks ($\sim$5 min and $\sim$10 min). Moreover, as the aggregation continued, the peak at 10 min slowly decreased as the peak at 5 min increased. This indicated that the 10-min peak consisted of smaller Aβ_{1-42} aggregates than the 5-min peak.

Although larger aggregates would typically be expected to migrate more slowly than smaller species, a previous study by Wang *et al.* has shown that Aβ_{1-42} aggregates exhibit a higher surface charge which would decrease their migration time and therefore explain why those peaks would be detected first.[44] To provide an estimate of the specific sizes of various

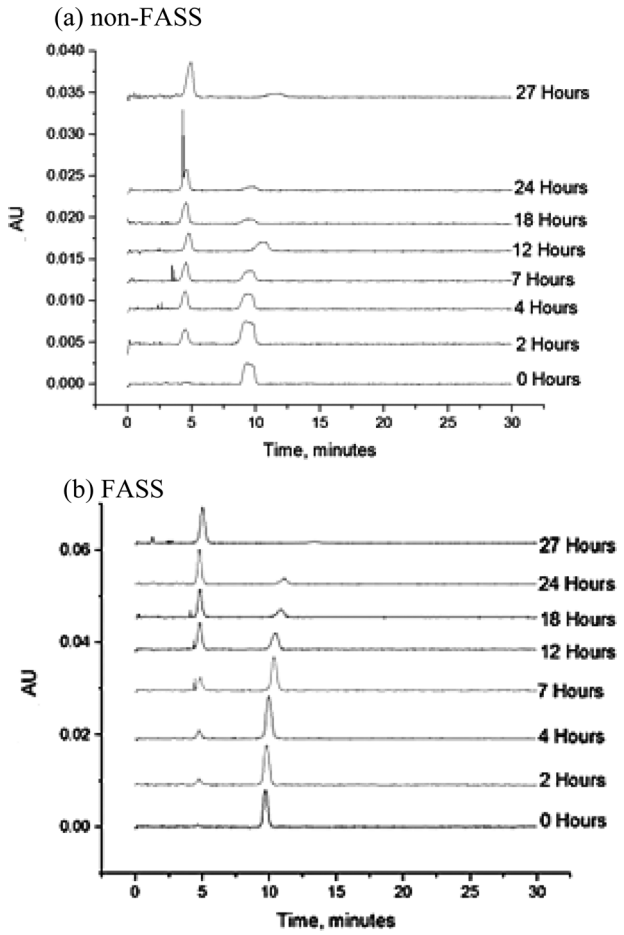

FIG. 2. Representative electropherograms for UV-CE detection of A$\beta_{1\text{-}42}$ aggregation using (a) non-FASS (100 mM sodium phosphate load buffer) and (b) FASS (40 mM sodium phosphate load buffer). The presence of very narrow peaks at or close to the 5-min peak were usually not replicated in experiments and were most likely due to microscopic bubbles.

Aβ species, multiple authors have previously used centrifugation.[24,30] Therefore, various molecular weights cutoff filters (300 kDa, 100 kDa, and 30 kDa) were used to provide an estimated molecular weight for the two species detected by UV-CE. The filtration studies (see supplementary material) provided an estimated size for the 10 min peak of less than 30 kDa (<7 mers) and for the 5 min peak between 30 and100 kDa (7–22 mers), which is within the size range of oligomeric species.[43]

As Fig. 2 shows, the peak patterns are very similar between the FASS and non-FASS conditions, but the peaks are much broader in the non-FASS conditions (Fig. 2(a)) than in the FASS conditions (Fig. 2(b)). Since the peak areas in electropherograms correlate to protein concentration, the changes in peak area during aggregation for both non-FASS and FASS conditions were determined as shown in Fig. 3. The changes in peak areas for both the <7 mers (Fig. 2(a)) and 7–22 mers (Fig. 2(b)) species were very similar throughout the aggregation process for both the non-FASS and FASS conditions. A previous study of the aggregation of HFIP treated A$\beta_{1\text{–}40}$ using UV-CE by Pryor *et al*. reported an initial increase in the smaller aggregates before a decrease was observed.[34] A similar pattern can be observed in Fig. 3(a) where the <7 mers species remain high or even increase in concentration, followed by a significant decrease at around 12–18 h of aggregation.

For the 7–22 mers species (Fig. 3(b)), a statistically significant increase in peak area was observed after 2 h of aggregation for both non-FASS and FASS conditions. After approximately 7 h of aggregation, the amount of 7–22 mers seemed to reach a plateau. It is interesting to note

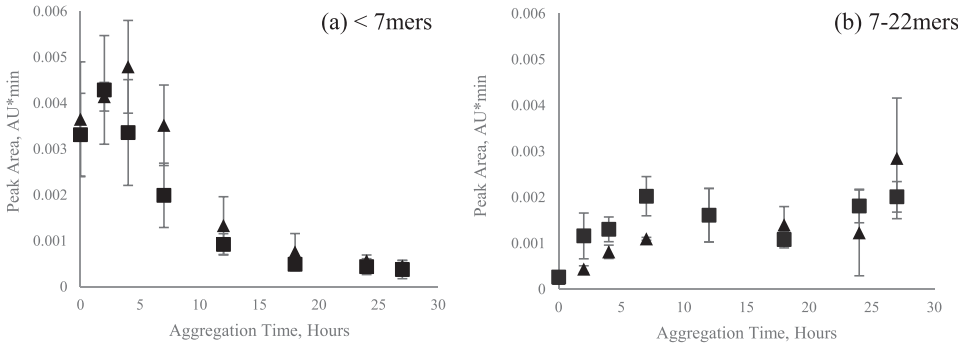

FIG. 3. Effect of FASS on with peak areas of Aβ1-42 oligomers detected using UV-CE. Peak area of (a) <7 mers (<30 kDa) and (b) 7–22 mers (30–100 kDa) oligomer species under non-FASS (■) and FASS (▲) conditions, n = 3.

that at 7 h (FASS) and 12 h (non-FASS), the peak areas for the <7 mers and 7–22 mers oligomeric species were statistically equal.

When comparing the peak areas between non-FASS and FASS conditions, the <7 mers species were statistically the same for all time points. For the 7–22 mers species, the non-FASS conditions had a statistically larger peak area than the FASS conditions between 2 and 7 h of aggregation. This could indicate that the lower ionic strength used in the FASS conditions led to a lower production of oligomeric species. However, formation of these early species can also be highly stochastic, which could be another source of the difference. It is interesting to note that the FASS conditions produced less statistical variation in the peak areas between 2 and 7 h of aggregation. By 12 h of aggregation, the peak areas for non-FASS and FASS conditions became statistically the same and remained so for the rest of the experimental analysis time (27 h). While there were some small differences in aggregation between the non-FASS and FASS conditions, overall they were very similar in terms of the aggregation time and concentration for the different oligomeric species.

Once it was established that FASS conditions did not dramatically alter the aggregation mechanism, it was important to characterize if FASS was having an impact on other important variables including peak height, peak width, and resolution. A$\beta_{1–42}$ can be expensive to purchase and difficult to obtain from physiological samples. Therefore, the ability to decrease the amount of A$\beta_{1–42}$ required for detection was desirable. By utilizing the FASS method, the peak height statistically increased for the <7 mers species (Fig. 4(a)) for all but two time points (12 and 24 h). For the 7–22 mers species, the peak height was statistically higher between 12 and 24 h of aggregation when using FASS and statistically the same as the non-FASS conditions for the remaining time points. Performing an average over all the species and time points, FASS yielded an increase in peak height of >60%.

It was also desirable for peak widths to be minimized as this improves the separation between the peaks and allows for potentially more species to be visualized. The FASS method had decreased peak widths for all but one aggregation time point (12 h) when analyzing the <7 mers species (Fig. 4(c)). For the 7–22 mers species, FASS produced statistically smaller peak widths for half of the time points and was statistically the same for the remaining time points (Fig. 4(d)). Performing an average over all the species and time points, FASS yielded a decrease in peak width of >75%.

Resolution is a measure of the quality of separation between the peaks and is a function of the peak width and the separation between the peaks. The resolution, RES, was determined by[26]

$$RES = \frac{2(x_1 - x_2)}{(w_{1,1} + w_{1,2}) + (w_{2,1} + w_{2,2})}, \tag{1}$$

where $w_{1,1}$ and $w_{1,2}$ are the bi-Gaussian widths for the first peak, $w_{2,1}$ and $w_{2,2}$ are the widths for the second peak, and x_1 and x_2 are the migration time for the respective peaks. For all aggregation time points, using FASS for UV-CE increased the resolution between the

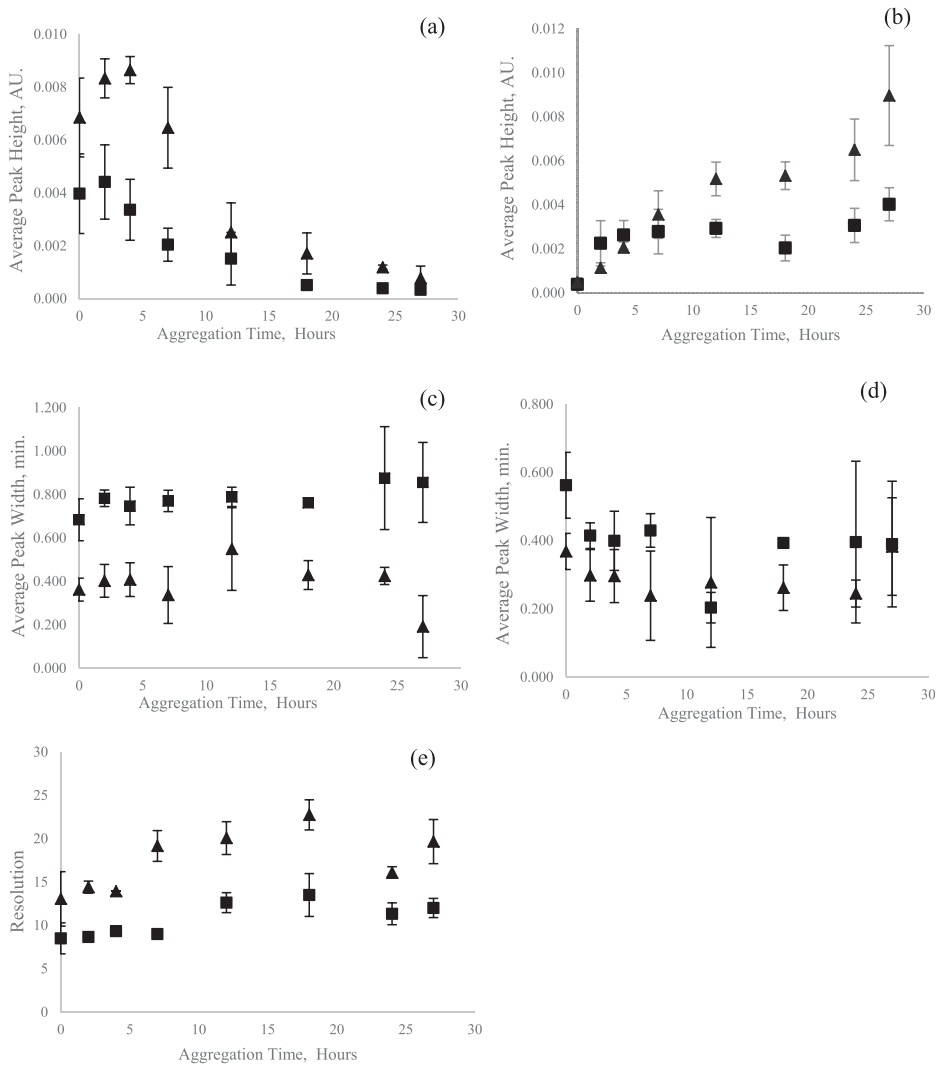

FIG. 4. Effect of FASS on peak height, peak width, and resolution of A$\beta_{1\text{-}42}$ oligomers detected using UV-CE. Non-FASS (■) and FASS (▲) analysis of <7 mers (a) peak height and (c) peak width compared to 7–22 mers (b) peak height and (d) peak width. (e) Resolution difference between the <7 mers and 7–22 mers for non-FASS (■) and FASS (▲) conditions. N = 3 for all experiments.

oligomeric species (Fig. 4(e)). For analysis of the aggregation of A$\beta_{1\text{–}42}$, FASS conditions provided better resolution, smaller peak widths, and larger peak heights for detection of the aggregating species. Therefore, FASS can be used to enhance the detection of aggregating proteins such as A$\beta_{1\text{–}42}$.

C. Congo red and Orange G inhibition

Although filtration studies were used to estimate the size of the aggregated species, they do not provide any information on their conformation. Therefore, Congo red and Orange G inhibition studies were conducted to further investigate the nature of these aggregates. Congo red has been reported to inhibit oligomer Aβ species or at least species smaller than fibrils.[41,45] Orange G has been reported to inhibit fibrils and to bind Aβ in such a manner that it does not stop monomers from aggregating but delays or eliminates fibril formation.[41] As shown in Fig. 5(a), Orange G did not inhibit the growth of the 7–22 mers peak, but instead appeared to increase the peak areas for both the <7 mers and 7–22 mers species during the course of the aggregation. This was further confirmed by comparing the peak areas with Fig. 3(a) where by 27 h the

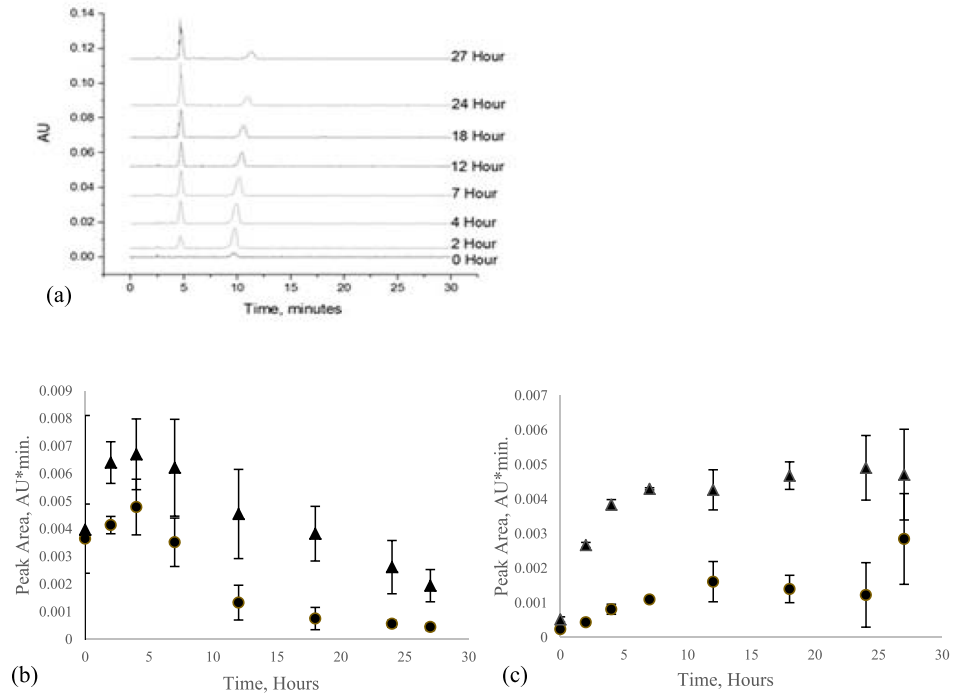

FIG. 5. Effect of Orange G inhibitor on A$\beta_{1\text{-}42}$ oligomers detected using UV-CE. (a) Representative electropherograms for A$\beta_{1\text{-}42}$ aggregated in the presence of Orange G. UV-CE with FASS peak areas for (b) <7 mers and (c) 7–22 mers without addition of inhibitor (●) or in the presence of inhibitor (▲) conditions, n = 3.

<7 mers aggregates decreased and the 7–22 mers species increased. Additionally, for both the <7 mers and 7–22 mers species, the peak areas in the Orange G inhibited samples were larger for the majority of time points compared to the uninhibited samples (Figs. 5(b) and 5(c)). While Orange G does give off a weak UV signal in the spectrum being used for detection, it was more likely that these larger peaks areas corresponded to the inability of larger species (specifically fibrils) to be formed in the presence of Orange G. This was further confirmed by TEM imaging where little to no pro-fibril and fibrils were observed in the presence of Orange G at these aggregation times. Interestingly, A$\beta_{1\text{–}42}$ inhibited with Orange G showed a significant amount of "circular" aggregates (see supplementary material).[43] Therefore, the species observed by UV-CE detection were smaller than fibrils.

While it was expected that the addition of Congo red would suppress the growth of the 7–22 mers species, the actual effect proved to be more complex. In half the experiments, Congo red inhibited the formation of the 7–22 mers species (Fig. 6(a)) while in the other half there did not appear to be any significant inhibition (Fig. 6(b)). When taking a closer look at the peak areas for the <7 mers (Fig. 6(c)) the trends were the same for the uninhibited sample as well as Congo Red inhibited samples. Interestingly, the samples that did not show significant inhibition of the 7–22 mers species have the highest peak areas for the <7 mers species. For the 7–22 mers samples, the Congo red samples that showed inhibition had almost no change in the peak area; alternatively, the Congo red samples that did not show inhibition exhibited an initial rapid increase in peak area. These samples also exhibited higher peak areas than the uninhibited samples at almost all aggregation time points. Congo red is considered a weak inhibitor which could explain its high level of variability between the different samples especially in the presence of a significant amount of larger aggregates at 0 h.[46] In addition, the larger initial amount of 7–22 mers species present in the samples could be acting as seeds for the growth of oligomers and thereby bypassing the species that Congo red typically inhibits. TEM imaging showed no change in the formation of fibrils between the uninhibited and Congo red inhibited samples (see supplemental material).[43] However, no proto-fibrils were observed in the Congo red

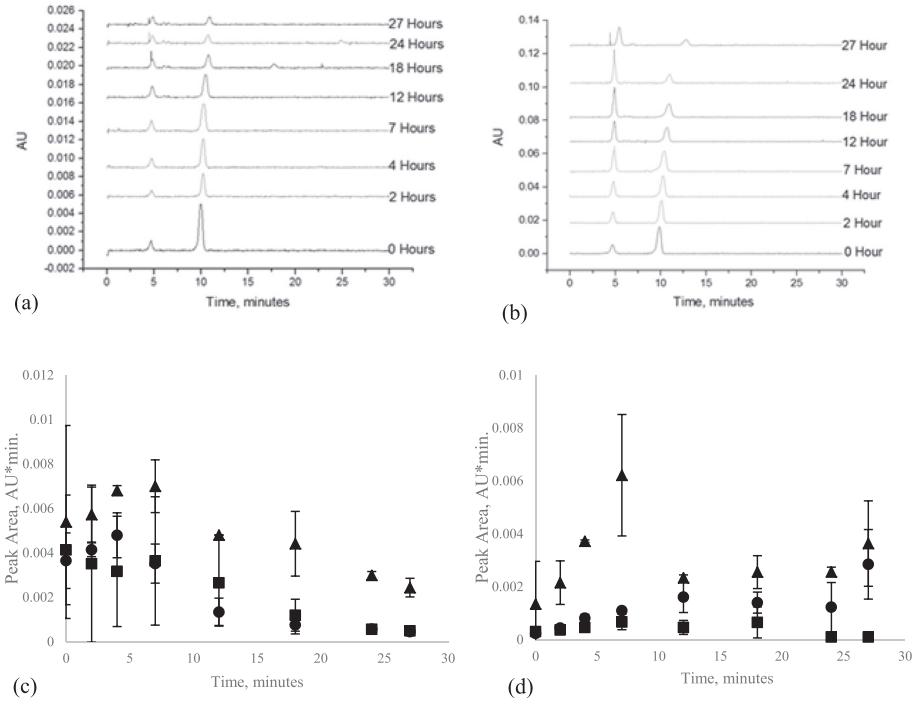

FIG. 6. Effect of Congo red inhibitor on A$\beta_{1\text{-}42}$ oligomers detected using UV-CE. Representative electropherograms for A$\beta_{1\text{-}42}$ aggregated in the presence of Congo Red showing (a) inhibition and (b) no inhibition. UV-CE with FASS peak areas for (c) <7 mers and (d) 7–22 mers without addition of inhibitor (●), with inhibitor but not showing inhibition (▲), or with inhibitor and showing inhibition (■) conditions, n ≥ 2.

inhibited samples and the smallest observable species appeared to have a different conformation in the Congo red samples compared to the uninhibited samples. The Congo red data indicated that the A$\beta_{1\text{–}42}$ species observed by UV-CE are most likely oligomers, although a stronger oligomer inhibitor would be recommended for future studies.

IV. CONCLUSION

This study demonstrated that UV-CE can be used to observe the early stages of A$\beta_{1\text{–}42}$ aggregation. These studies were conducted without the use of denaturants or organic solvents which have been reported to alter the native aggregation of Aβ. By employing FASS with UV-CE, a higher resolution separation with larger peak intensities (>60% average increase) and smaller peak widths (>75% average reduction) was achieved without significant alteration to the aggregation process. While conducting the FASS technique using the CE, it was also important to ensure the A$\beta_{1\text{–}42}$ aggregation was not affected by varying sample buffer compared to the BGE. The peak areas for the non-FASS and FASS conditions were statistically similar for the majority of the time points. Filtration experiments were used to estimate that the species detected were <7 mers (<30 kDa) and 7–22 mers (30–100 kDa). Inhibition experiments with Congo red and Orange G indicated that the species observed by UV-CE were smaller than fibrils and most likely oligomeric. Overall this study shows the promise of using a pre-concentration technique such as FASS to enhance the ability of UV-CE to study the early stages of amyloid aggregation.

ACKNOWLEDGMENTS

This publication was supported by Grant Nos. 1P30RR031154-02 and 8P30GM103450-03 from the National Center for Research Resources (NCRR), a component of the National Institutes of Health (NIH), by the Arkansas Biosciences Institute, the major research component of the Arkansas Tobacco Settlement Proceeds Act of 2000, and by a grant from the Alzheimer's

Association (NIRP-12-258371). In addition, the authors would like to thank Tammy Lutz-Rechtin, Betty Martin, and Phillip Turner for their technical assistance as well as acknowledging the use of Arkansas Nano & Bio Materials Characterization Facility at the University of Arkansas, supported by the National Science Foundation and the State of Arkansas.

[1]A. Yam, X. Wang, C. Gao, M. Connolly, R. Zuckermann, T. Blue, J. Hall, J. Fedynyshyn, S. Allauzen, D. Peretz, and C. Salisbury, Biochemistry **50**, 4322 (2011).
[2]D. Whitford, *Proteins: Structure and Function* (Wiley, 2005), p. 426.
[3]I. W. Hamley, Chem. Rev. **112**, 5147 (2012).
[4]D. J. Selkoe, Science **298**, 789 (2002).
[5]R. Murphy, Biochim. Biophys. Acta **1768**, 1923 (2007).
[6]Alzheimer's Association, 2015 Alzheimer's Disease Facts and Figures, Alzheimer's Association, 2015.
[7]O. El-Agnaf, D. S. Mahil, B. P. Patel, and B. M. Austen, Biochem. Biophys. Res. Commun. **273**, 1003 (2000).
[8]F. LaFerla, Biochem. Soc. Trans. **38**, 993 (2010).
[9]T. Paul, K. O'Connor, W. P. Tate, and W. C. Abraham, Prog. Neurobiol. **70**, 1 (2003).
[10]C. M. Gao, A. Y. Yam, X. Wang, E. Magdangal, C. Salisbury, D. Peretz, R. N. Zuckermann, M. D. Connolly, O. Hansson, L. Minthon, H. Zetterberg, K. Blennow, J. P. Fedynyshyn, and S. Allauzen, PLoS One **5**, e15725 (2010).
[11]D. Rosenman, C. Connors, W. Chen, C. Wang, and A. E. Garcia, Mol. Biol. **425**, 3338 (2013).
[12]P. Jingxi, J. Han, C. H. Borchers, and L. Konermann, Biochemistry **51**, 3694 (2012).
[13]T. Iwatsubo, A. Odaka, N. Suzuki, H. Mizusawa, N. Nukina, and Y. Ihara, Neuron **13**, 45 (1994).
[14]M. Ahmed, J. Davis, D. Aucoin, T. Sato, S. Ahuja, S. Aimoto, J. I. Elliott, W. E. Van Nostrand, and S. O. Smith, Nat. Struct. Mol. Biol. **17**, 561 (2010).
[15]M. Yang and D. Teplow, J. Mol. Biol. **384**, 450 (2008).
[16]S. Weggne, J. L. Eriksen, P. Das, S. Sagi, R. Wang, C. Pietrzik, K. A. Findlay, T. E. Smith, M. P. Murphy, T. Bulter, D. Kang, N. Marquez-Sterling, T. Golde, and E. Koo, Nature **414**, 212 (2001).
[17]P. N. Lacor, M. C. Buniel, P. W. Furlow, A. S. Clemente, P. T. Velasco, M. Wood, K. L. Viola, and W. L. Klein, J. Neurosci. **27**, 796 (2007).
[18]C. Haass and D. J. Selkoe, Nat. Rev. Mol. Cell Biol. **8**, 101 (2007).
[19]G. Bitan, A. Lomakin, and D. B. Teplow, J. Biol. Chem. **276**, 35176 (2001).
[20]L.-F. Lue, Y. M. Kuo, A. E. Roher, L. Brachova, Y. Shen, L. Sue, T. Beach, J. H. Kurth, R. E. Rydel, and J. Rogers, Am. J. Pathol. **155**, 853 (1999).
[21]A. J. Miñano-Molina, J. Espana, E. Martin, B. Barneda-Zahonero, R. Fado, M. Sole, R. Trullas, C. A. Saura, and J. Rodriquez-Alvarez, J. Biol. Chem. **286**, 27311 (2011).
[22]A. Laganowsky, C. Liu, M. R. Sawaya, J. P. Whitelegge, J. Park, M. Zhao, A. Pensalfini, A. B. Soriaga, M. Landau, P. K. Teng, D. Cascio, C. Glabe, and D. Eisenberg, Science **335**, 1228 (2012).
[23]R. Kayed, A. Pensalfini, L. Margol, Y. Sokolov, F. Sarsoza, E. Head, J. Hall, and C. Glabe, J. Biol. Chem. **284**, 4230 (2009).
[24]E. Pryor, M. Moss, and C. Hestekin, J. Mol. Sci. **13**, 3038 (2012).
[25]R. Kayed, E. Head, F. Sarsoza, T. Saing, C. W. Cotman, M. Necula, L. Margol, J. Wu, L. Breydo, J. L. Thompson, S. Rasool, T. Gurlo, P. Butler, and C. G. Glabe, Mol. Neurodegener. **2**, 18 (2007).
[26]J. P. Landers, *Handbook of Capillary Electrophoresis* (CRC Press LLC, Florida, 1997).
[27]M. Breadmore, J. Chromatogr. A **1221**, 42 (2012).
[28]N. A. Lacher, K. E. Garrison, R. S. Martin, and S. M. Lunte, Electrophoresis **12**, 2526 (2001).
[29]S. F. Y. Li and L. J. Kricka, Clin. Chem. **52**, 37 (2006).
[30]S. Sabella, M. Quaglia, C. Lanni, M. Racchi, S. Govoni, G. Caccialanze, A. Calligaro, V. Bellotti, and E. De Lorenzi, Electrophoresis **25**, 3186 (2004).
[31]R. A. Picou, I. Kheterpal, A. Wellman, M. Minnamreddy, G. Ku, and S. D. Gilman, J. Chromatogr. B **879**, 627 (2011).
[32]M. Kato, H. Kinoshita, M. Enokita, Y. Hori, T. Hashimoto, T. Iwatsubo, and T. Toyo'oka, Anal. Chem. **79**, 4887 (2007).
[33]D. Brambilla, R. Verpillot, M. Taverna, L. De Kimpe, B. Le Droumaguet, J. Nicolas, M. Canovi, M. Gobbi, F. Mantegazza, M. Salmona, V. Nicolas, W. Scheper, P. Couvreur, and K. Andrieux, Anal. Chem. **82**, 10083 (2010).
[34]N. E. Pryor, M. Moss, and C. Hestekin, Electrophoresis **35**, 1814 (2014).
[35]M. R. Mohamadi, Z. Svobodova, R. Verpillot, H. Esselmann, J. Wiltfang, M. Otto, M. Taverna, Z. Bilkova, and J.-L. Viovy, Anal. Chem. **82**, 7611 (2010).
[36]H. Schwartz and T. Pritchett, *Separation of Proteins and Peptides by Capillary Electrophoresis: Application to Analytical Biotechnology* (Fullerton, 1992).
[37]D. Osbourn, D. Weiss, and C. Lunte, Electrophoresis **21**, 2768 (2000).
[38]F. Kitagawa and K. Otsuka, J. Chromatogr. A **1335**, 43 (2014).
[39]V. Dolník and K. M. Hutterer, Electrophoresis **22**, 4163 (2001).
[40]C.-H. Lin and T. Kaneta, Electrophoresis **25**, 4058 (2004).
[41]M. Necula, R. Kayed, S. Milton, and C. G. Glabe, J. Biol. Chem. **282**, 10311 (2007).
[42]C. Hestekin, J. P. Jakupciak, T. N. Chiesl, C. W. Kan, C. D. O'Connell, and A. E. Barron, Electrophoresis **27**, 3823 (2006).
[43]See supplementary material at http://dx.doi.org/10.1063/1.4954051 for the TEM method and images, Tht assay information, and CE filter data.
[44]Q. Wang, N. Shah, J. Zhao, C. Wang, C. Zhao, L. Liu, L. Li, F. Zhou, and J. Zheng, Phys. Chem. Chem. Phys. **13**, 15200 (2011).
[45]K. Yokoyama, A. D. Fisher, A. R. Amori, D. R. Welchons, and R. E. McKnight, J. Biophys. Chem. **1**, 153 (2010).
[46]S. K. Pachahara, N. Chaudhary, C. Subbalakshmi, and R. Nagaraj, J. Pept. Sci. **18**, 233 (2012).